J Solid State Electrochem (2006) 10:934–940
DOI 10.1007/s10008-006-0153-8

ORIGINAL PAPER

Electrical and electro-chemical characterisation of $La_{0.99}Fe_{1-x}Ni_xO_{3-\delta}$ perovskites

K. Kammer · L. Mikkelsen · J. B. Bilde-Sørensen

Received: 23 February 2006 / Revised: 15 March 2006 / Accepted: 7 April 2006 / Published online: 31 May 2006

Abstract $La_{0.99}Fe_{1-x}Ni_xO_{3-\delta}$ (LFN, $0<x<0.6$) perovskites were synthesised by a solid-state route and were characterised by powder XRD, dilatometry, four-point DC conductivity measurements and electro-chemical impedance spectroscopy (EIS) on cone-shaped electrodes using a $Ce_{1.9}Gd_{0.1}O_{1.95}$ (CGO10) electrolyte. All the compounds were of single phase, and they belong to either the cubic or the hexagonal crystal system. The thermal expansion coefficient (TEC) was in the range $10.7*10^{-6}$ K^{-1} to $13.4*10^{-6}$ K^{-1}, which continued to increase with increasing nickel content. The highest electronic conductivity was measured for the composition $La_{0.99}Fe_{0.4}Ni_{0.6}O_{3-\delta}$, giving a value of 670 S/cm at 380 °C. The highest electro-chemical performance was measured for the composition $La_{0.99}Fe_{0.4}Ni_{0.6}O_{3-\delta}$ giving an area specific resistance as low as 5.5 Ωcm^2 at 600 °C based on EIS measurements on a cone-shaped electrode. Composite cathodes made from $La_{0.99}Fe_{0.4}Ni_{0.6}O_{3-\delta}$ and CGO10 revealed a rather low performance due to an un-optimised micro-structure.

Introduction

The solid oxide fuel cell (SOFC) is a convenient and an environmentally friendly pathway to the simultaneous generation of heat and electricity [1]. One major obstacle in the commercialisation of the SOFC is the relative high operation temperature [2]. For lowering of the operation temperature of the SOFC, new cathode materials are needed.

K. Kammer (✉) · L. Mikkelsen · J. B. Bilde-Sørensen
Department of Fuel Cells and Solid State Chemistry,
Risø National Laboratory,
4000 Roskilde, Denmark
e-mail: kent.kammer.hansen@risoe.dk

In the literature, most attention has been paid to the perovskites $La_{0.6}Sr_{0.4}Fe_{0.8}Co_{0.2}O_{3-\delta}$ and $Sm_{0.5}Sr_{0.5}CoO_{3-\delta}$ made as composite cathodes with ceria-based electrolyte powder [3–8]. The best performance obtained appears to be 0.18 Ωcm^2 at 600 °C for an $Sm_{0.5}Sr_{0.5}CoO_{3-\delta}$/CGO10 composite cathode on a ceria-based electrolyte [5]. Recently, even lower area specific resistance (ASR) values have been obtained with a $Ba_{0.5}Sr_{0.5}Fe_{0.2}Co_{0.8}O_{3-\delta}$-based cathode [9]. The main concern with this type of electrodes is, however, that the Co or Fe–Co-based perovskites react with zirconia-based electrolytes, forming insulating layers between the electrolyte and the cathode [6]. Another problem is a high thermal expansion coefficient (TEC) that do not match the TEC of zirconia-based electrolytes, limiting the possibility of temperature cycles [10].

Another potential cathode for low temperature operation of the SOFC is $LaFe_{1-x}Ni_xO_{3-\delta}$-based perovskites which have a high electronic conductivity and a TEC matching the other cell components of the SOFC [11–13]. Chiba et al. [11] investigated porous planar electrodes of some LFN compounds. The best performance was measured for the composition $LaFe_{0.4}Ni_{0.6}O_3$ with an ASR value of 0.028 Ωcm^2 at 800 °C. Furthermore, several authors have undertaken conductivity measurements, and the electronic conductivity is very high especially for the composition $LaFe_{0.4}Ni_{0.6}O_{3-\delta}$ [11–14]. The electronic conductivity of this compound reaches a maximum value of 580 S/cm at a temperature of 800 °C [12]. Literature data on the crystal structure of $LaFe_{1-x}Ni_xO_{3-\delta}$ perovskites are diverse [11–17]. In the work of Bontempi et al. [15], a tentative phase diagram is presented for some LFN perovskites. The LFN perovskites belong to either the cubic or the orthorhombic crystal system, depending on the temperature. Below 850 °C, the LFN perovskites with low amounts of Ni are cubic. Above 850 °C, the LFN perovskites belong to the

Table 1 The matrix for the evaluation of the electro-chemical performance of the $La_{0.99}Fe_{0.4}Ni_{0.6}O_{3-\delta}$ compound: the composition of the composite cathodes given in weight percent with the amount of the perovskite phase listed first

Temperature (°C)	900	950	1,000	1,050
Composition	50/50 (3)	50/50 (1)	50/50 (5)	50/50 (6)
Composition		60/40 (2)		
Composition		70/30 (4)		

The calcination temperature of the cathodes is given in the header. The numbers of the samples are given in parentheses

orthorhombic crystal system. The Ni-rich LFN perovskites undergo a phase transition (cubic to orthorhombic) at a lower temperature (approximately 750 °C) according to Bontempi et al. [15]. In the paper of Falcón et al. [16], it is stated that LFN perovskites with x between 0.0 to 0.5 are orthorhombic and LFN perovskites with x between 0.5 to 1.0 are rhombohedral. Together this shows that the thermal history of the perovskites determines the crystal structure of the perovskites.

The TEC of the LFN perovskites has been measured by several authors [12, 14, 17], and it is in the range of 9.5 to $13.3*10^{-6}$ K^{-1} from room temperature to 1,000 °C, depending on the composition and the study. The TEC increases with increasing nickel content. In the study of Chiba et al. [12], it is stated that the TEC of the composition $LaFe_{0.4}Ni_{0.6}O_{3-\delta}$ is $11.3*10^{-6}$ K^{-1}, whereas it is stated to be $12.1*10^{-6}$ K^{-1} in the study of Basu et al. [14]. The difference in the measured TEC of LFN perovskites might be due to differences in the density of the samples used for the dilatometry measurements.

In this work, seven $La_{0.99}Fe_{1-x}Ni_xO_{3-\delta}$ ($0<x<0.6$) perovskites were characterised by powder XRD, dilatometry, four-point DC conductivity measurements and electrochemical impedance spectroscopy (EIS) on cone-shaped electrodes. The small A-site deficiency was chosen to ensure that the perovskites were slightly A-site deficient. In the case of an aimed A/B ratio of unity, one can never be sure whether the perovskites are over- or under-stoichiometric. From literature, it is known that NiO but not Fe_2O_3 is expelled from the perovskite phase when the LFN perovskites are attempted to be synthesised with an A/B ratio less than unity [13].

The idea behind the use of cone-shaped electrodes is that it eliminates some of the problems encountered with porous planar electrodes. That is, the contact area between the electrolyte and the cone-shaped electrode is well defined. The contact area can be calculated using Newman's formula [18]:

$$r = \frac{1}{4R_s\sigma^*} \quad , \tag{1}$$

where r is the radius of the contact point, R_s is the high-frequency intercept in the complex plane with the real axis in the impedance plot and σ^* is the specific conductivity of the electrolyte. The method is particularly well suited for a direct comparison of different electrode materials, as is the case in this study.

Symmetrical cells with composite cathodes of $La_{0.99}Fe_{0.4}Ni_{0.6}O_{3-\delta}$ and CGO10 were also evaluated with EIS.

The aim of this study is to re-investigate the performance of LFN perovskites as SOFC cathodes using the cone-shaped electrode method. This is done to see if whatever the results published in the work of Chiba et al. [11] could be re-produced using the cone-shaped electrode technique, or if the cone-shaped electrode gives different results. The cone-shaped electrode technique is less sensitive to the micro-structure of the electrodes than electro-chemical investigations on porous planar electrodes.

Experimental

Synthesis of the seven $La_{0.99}Fe_{1-x}Ni_xO_{3-\delta}$ perovskites was performed by a solid-state reaction route, where powders of La_2O_3, Fe_2O_3 and NiO were mixed in the appropriate ratios and ball-milled for 24 h in EtOH with zirconia balls. The powders were calcined twice for 12 h at 1,200 °C with intermediate ball milling. The phase purity of the powders was checked by powder XRD, using a Stoe diffractometer with $Cu_{K\alpha}$ radiation. Cylinders and bars were pressed in appropriate dies and sintered for 12 h at 1,400 °C before they were machined into cone-shaped electrodes with height and diameter measuring 7.5 mm, and bars of an approximate size of 4*4*18 mm^3. The size of the contact between the electrolyte and the cone-shaped electrodes was around $5*10^{-5}$ cm^2 as determined by Newman's formula. The densities of the sintered samples were measured by the Archimedes method, and all the samples had a density above 95% of the theoretical density. The samples were equilibrated at 1,000 °C in air for 12 h before the measurements. The measurements of the TEC in air were

Table 2 Unit-cell parameters for $La_{0.99}Fe_{1-x}Ni_xO_{3-\delta}$ perovskites

x	0.0	0.1	0.2	0.3	0.4	0.5	0.6
A/Å	3.9286	3.9221	3.9118	3.8998	3.8906	3.8817	5.5001
C/Å							13.243

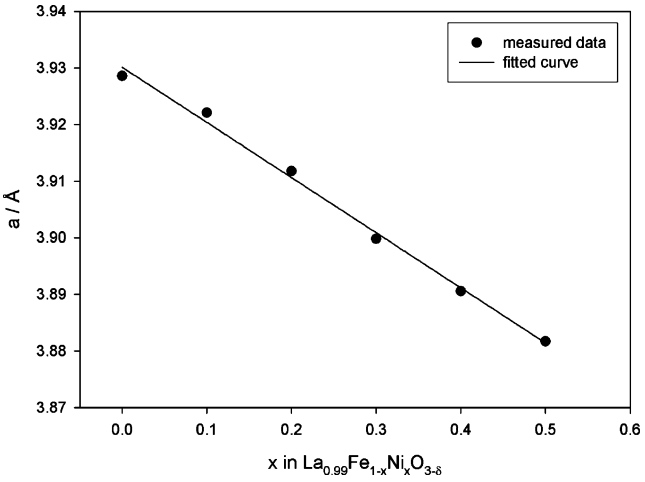

Fig. 1 Unit-cell parameters for the cubic perovskites plotted against the amount of nickel in $La_{0.99}Fe_{1-x}Ni_xO_{3-\delta}$. The unit-cell parameters decrease with increasing amount of nickel

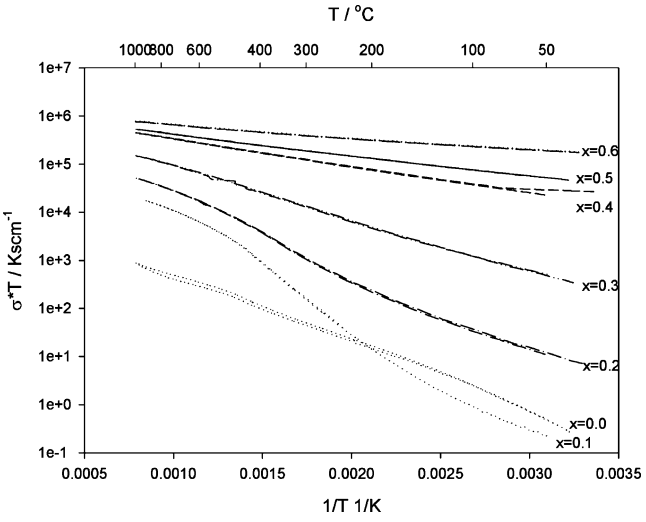

Fig. 2 Electrical conductivity of $La_{0.99}Fe_{1-x}Ni_xO_{3-\delta}$ perovskites from room temperature to 1,000 °C

made using a Setaram DHT 2050 K dilatometer with heating and cooling ramps of 2 °C/min up to 1,000 °C. Before cooling, the samples were equilibrated for 2 h at 1,000 °C. The four-point DC measurements were also measured on the bars as follows: The data were measured and collected with a PC-Keithley micro-ohmmeter set-up and an in-house software to collect the conductivity data and control the temperature. The heating and cooling ramps were 3 °C/min. The samples were heated in increments of 50 °C. The samples were kept at temperature for 2 h. Conductivity measurements were performed every fifth minute. EIS on the cone-shaped electrodes was recorded at 800, 700 and 600 °C using an amplitude of 24 mV and a frequency range of 1 MHz to 0.05 Hz, with five points measured at each decade. A Solartron 1260 gain-phase analyser was used for the measurements. The cone was kept for 1 day at each temperature before the measurements. The set-up was a single atmosphere set-up, and the measurements were performed in air. Approximately 100 g of weight was put on the cone during the measurements. A pellet of CGO10 was used as electrolyte. The reference/counter electrode consisted of silver metal (added as silver paste, Engelhard). The silver electrode was sintered in situ.

Porous symmetrical cells were produced by slurry spraying on CGO10 plates (InDEC BV, The Netherlands). The slurries were fabricated as follows: The $La_{0.99}Fe_{0.4}Ni_{0.6}O_{3-\delta}$ powder was mixed with CGO10 powder (Rhodia) in the ratios 50/50, 60/40 and 70/30 (*w*/*w* %/%). The powder mixture was then transferred to a PVC bottle and an appropriate binder was added together with ethanol. The slurries were ball-milled overnight. After ball milling, the slurries were sprayed on both sides of the CGO10 plates in two layers with intermediate sintering. The first layer had a thickness of approximately 10 μm, and the second layer had a thickness of approximately 15 μm. The symmetrical cells were sintered at either 900, 950, 1,000 or 1,050 °C for 2 h in air. The experimental matrix is given in Table 1 together with the number of the samples. The samples were cut into smaller pieces with a size of approximately 4*4 mm^2 before the measurements. Pt paste was added on top of the electrodes as a current collector. The samples were mounted in a rig with Pt meshes and a spring-loaded load. The measurements on the symmetrical cells were performed at 800, 700 and 600 °C with the same conditions as for the cone-shaped electrodes. The data were fitted using the PC-DOS program by Boukamp [19]. In general, as few components as possible were used for the fitting whilst still obtaining a solid fit. The micro-structure of the porous symmetrical composite cathodes was investigated using a JEOL LV-SEM.

Results

Powder XRD showed that the powders were of single phase. The nickel-rich perovskite was hexagonal, whereas

Table 3 TEC values for $LaFe_{1-x}Ni_xO_{3\delta}$ perovskites in air from 100 to 1,000 °C

x	0.0	0.1	0.2	0.3	0.4	0.5	0.6
TEC	10.7±0.2	11.2±0.1	11.6±0.2	11.7±0.3	13.2±0.1	13.3±0.2	13.4±0.2

TEC values are given in 10^{-6} K^{-1}

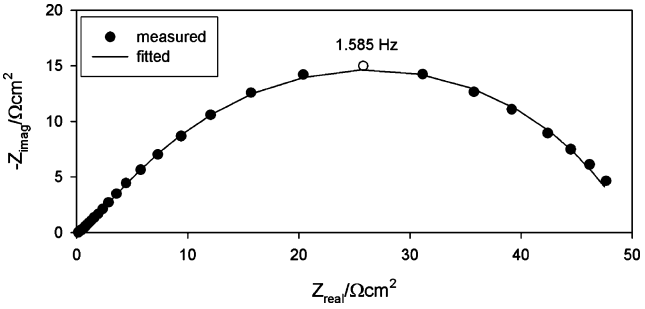

Fig. 3 EIS spectrum of an $La_{0.99}FeO_{3-\delta}$ cone recorded at 600 °C in air using a CGO10 electrolyte and silver metal as a counter/reference electrode. Fitted spectrum is shown as *solid line*

the other perovskites were cubic. The unit-cell parameters are shown in Table 2. The unit-cell parameters of the cubic phases are plotted in Fig. 1. It is observed that the size of the unit cell decreases with increasing nickel content. The results of the dilatometry measurements are shown in Table 3. It is a general trend that the TEC increases with increasing nickel content. The results of the four-point DC conductivity measurements are shown in Fig. 2. The conductivity is highest for the composition $La_{0.99}Fe_{0.4}Ni_{0.6}O_{3-\delta}$, and it reaches a maximum of 670 S/cm at 380 °C. Whereas this compound shows a maximum in conductivity at 380 °C, the other compounds show an increase in conductivity with increasing temperature. The nickel-free compound has only a very low electronic conductivity (the powder is brown, the other powders are black). In general, the electronic conductivity is very low from room temperature up to approximately 300 °C for the iron-rich compounds. The perovskites showed only a very small hysteresis in the conductivity upon heating and cooling.

An example of an EIS spectrum measured on a cone-shaped electrode of $La_{0.99}FeO_{3-\delta}$ is shown in Fig. 3. The spectrum consists of three arcs. This is difficult to see in the figure as the high-frequency arc is very small. The lowest ASR value is measured for the $La_{0.99}Fe_{0.4}Ni_{0.6}O_{3-\delta}$ composition, and is approximately 5.5 Ωcm^2 at 600 °C. It is also noteworthy that the ASR value for the nickel-free perovskite $La_{0.99}FeO_{3-\delta}$ is lower than for several of the nickel-containing perovskites. All the ASR values obtained on the cone-shaped electrodes are given in Table 4.

The ASR values measured on the symmetrical cathodes can be found in Table 5 and in Figs. 4 and 5. The lowest ASR value measured was measured for sample 1, giving a value of 0.73 Ωcm^2 at 800 °C. An example of an SEM micrograph of the symmetrical cathodes is shown in Fig. 6, for the sample numbered 4. The SEM picture reveals that one of the two phases has a very large particle size. This phase was identified as the perovskite phase by energy dispersive spectroscopy (EDS). This is the case for all the samples. Furthermore, there is no percolation pathway between the perovskite particles.

Discussion

The powder XRD reveals as expected a smaller size of the unit cell for the nickel-rich than for the nickel-poor perovskites because 6-coordinated Ni(III) has a smaller ionic radius than 6-coordinated Fe(III). The decrease in unit-cell parameters with increasing nickel content for the cubic compounds follows Vegard's law as seen in Fig. 1. The structure of most of the perovskites is cubic, in contrast to what is found in the study of Chiba et al. [12] where the perovskites are indexed in the orthorhombic crystal system. This can be due to differences in the heat treatment of the perovskites powders, which can affect the amount of oxide ion vacancies in the perovskite structure, because of slow kinetics/adjustment of the oxygen stoichiometry. This will lead to differences in the crystal structure of the perovskites. Different crystal structures of LFN perovskite are also reported in the literature.

The reason for the increased expansion, of the perovskite during heating, with increasing nickel content is probably due to the Jahn–Teller distortion induced by the d^7 Ni(III) ion. The values found in this study are close to the values of the commonly used zirconia-based electrolytes [1]. The TEC values found in this study are higher than the values found in the study of Chiba et al. [12].

The electrical conductivity is strongly dependent on the amount of Ni in the samples. The highest electronic conductivity is reached in the compound with the highest Ni content. The reason for an increase in the electronic conductivity when doping with nickel is due to the reaction:

$$Fe_{Fe}^{x} + Ni_{Fe}^{x} \leftrightarrow Fe_{Fe}^{\bullet} + Ni_{Fe}^{\prime} \; . \qquad (2)$$

This creates a mixed valence compound where the electron can jump between the transition metals with

Table 4 The ASR values of cones of $La_{0.99}Fe_{1-x}Ni_xO_{3-\delta}$ compounds measured at three different temperatures

x/temp.	0.0	0.1	0.2	0.3	0.4	0.5	0.6
600 °C	50	120	95	72	40	10	5.5
700 °C	10.2	48.7	14.6	9.2	4.0	0.80	0.76
800 °C	0.5	6.76	0.87	0.77	0.54	0.13	0.10

The ASR values are given in Ωcm^2

Table 5 The ASR values of composite electrodes given in Ωcm^2 at three different temperatures

Number/temp.	1	2	3	4	5	6
600 °C	25.6	40.6	32.2	10.2	39.2	120
700 °C	3.30	7.84	7.20	4.00	7.10	14.0
800 °C	0.73	2.88	1.84	1.20	1.52	2.54

different oxidation stages leading to a high electronic conductivity. For the $La_{0.99}Fe_{0.4}Ni_{0.6}O_{3-\delta}$ compound, the conductivity increases until a temperature of 380 °C, after which it decreases. This might be due to reduction of the perovskite leading to creation of oxide ion vacancies:

$$O_O^x + 2Ni_{Fe}^x \leftrightarrow 2Ni_{Fe}^{'} + V_O^{\bullet\bullet} + \tfrac{1}{2} O_2(g). \quad (3)$$

The creation of oxide ion vacancies in the perovskite structure leads to a decoupling of the transition metal–oxygen–transition metal super-exchange interactions, which lowers the electronic conductivity of the perovskites. However, if this was true, the dilatometry curve should bend at 380 °C (expansion upon reduction), and that is not the case. Therefore, it is probably an indication of a change in the conductivity mechanism at 380 °C for the $La_{0.99}Fe_{0.4}Ni_{0.6}O_{3-\delta}$ compound. One explanation could be that the conductivity mechanism is $LaFeO_3$-like (small polaron hopping between iron cations [20, 21]) below 380 °C and $LaNiO_{3-\delta}$-like (metallic conductivity due to overlap between 3d transition metal orbitales and oxygen 2p orbitales [22]) above 380 °C. The conductivities measured in this study are in general higher than the ones reported in the literature. This might be due to the higher symmetry observed for the perovskites used in this investigation compared with the perovskites reported in the literature. A higher symmetry gives a larger overlap between transition metal 3d orbitales and oxygen 2p orbitales leading to a higher electronic conductivity as mentioned before. The bending of the bonding angle is smaller when the symmetry is high.

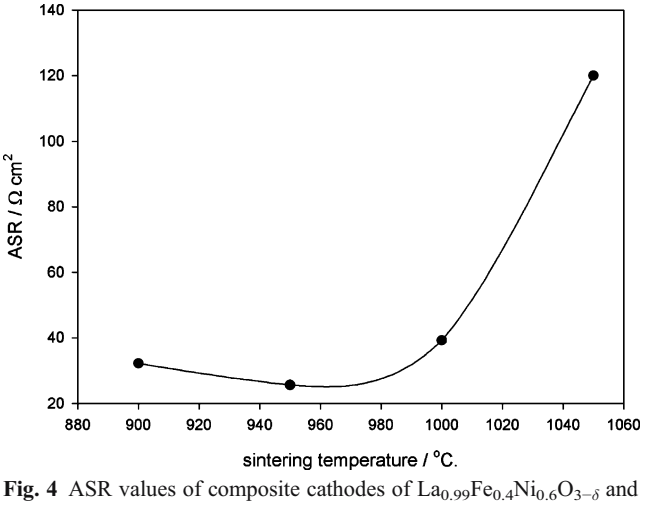

Fig. 4 ASR values of composite cathodes of $La_{0.99}Fe_{0.4}Ni_{0.6}O_{3-\delta}$ and CGO10 at 600 °C as a function of sintering temperature. The lowest ASR value is reached for the electrode sintered at 950 °C

The trend found in this study for the ASR values as a function of nickel content is the same as found in the literature [11], except for the pure iron compound. The dependence of the ASR with nickel contents is probably due to a high amount of oxygen vacancies for the nickel-rich compounds. Oxygen vacancies are generally accepted to be the catalytic active sites for the reduction of oxygen [23]. Furthermore, the samples with high nickel content contains more Fe(IV) than the iron-rich compounds due to reaction (Eq. 2). In literature, it is sometimes stated that Fe (IV) may be more active for the reduction of oxygen than Fe(III) [24]. That the performance of the pure iron compound is higher than for several of the Ni-containing samples is, in the light of this, therefore quite surprising (low conductivity, low or no amount of Fe(IV) and a low amount of oxide ion vacancies). However, this could be due to a pitfall in the experimental set-up [25]. The intercept at high frequency with the real axis in the impedance plot is given by the equation:

$$R_s = R_{elyt} + R_{cone}\,, \quad (4)$$

where R_{elyt} is the resistance of the electrolyte, and R_{cone} is the resistance of the cone, which often is negligible. However, if the cone has a very low electronic conductivity, the contribution of the cone leads to a lower contact area giving a wrong value of ASR compared with the other compounds. This can be corrected for if the resistance of the cone is known. The resistance of the cone can be calculated, as the electronic conductivity of the cone is known[1]. We used finite element calculations to calculate the resistance of the cone, using the program FEMLAB [26]. This gave a value of approximately 450 Ω for the cone at 600 °C (out of a total R_s of 3,300 Ω). This results in an increase in the contact area calculated by Newman's formula, giving an increase of the ASR at 600 °C to 67 Ωcm^2. This is still lower than for several of the Ni-

[1]The electronic conductivity of the cone could not be measured directly as the contact point differs from measurement to measurement. This gives a different resistance of the cone from measurement to measurement.

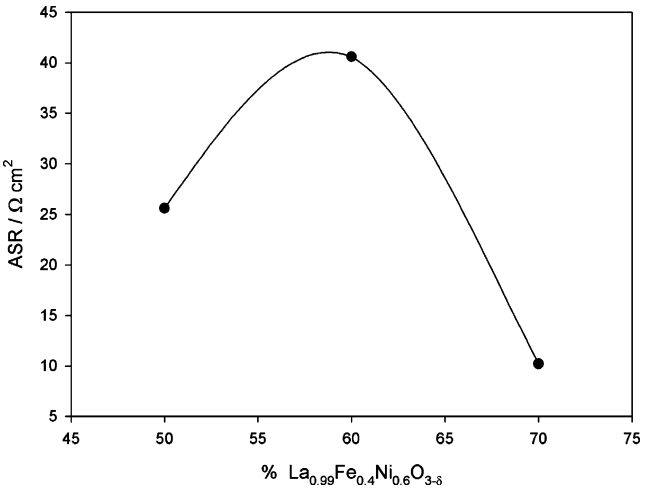

Fig. 5 ASR values of composite cathodes of $La_{0.99}Fe_{0.4}Ni_{0.6}O_{3-\delta}$ and CGO10 at 600 °C as a function of composition. The lowest ASR value is reached for the electrode containing 70 % perovskite

containing samples, and the relative low ASR value must therefore be a true material property of the $La_{0.99}FeO_{3-\delta}$ compound. A possible explanation for this is the following: Fe(III) can disproportionate according to the equation:

$$2Fe_{Fe}^{x} \rightarrow Fe_{Fe}^{\bullet} + Fe_{Fe}^{'} . \quad (5)$$

This means that $La_{0.99}FeO_3$ has the possibility to contain a small amount of Fe(IV). However, no sign of Fe(II) was found for similar compounds by Mössbauer spectroscopy [27]. Furthermore, defect chemistry modelling shows no sign of Fe(III) disproportionation [28]. The low electronic conductivity is also an indication that no charge disproportionation occurs. However, if Fe(III) is more catalytic active than Fe(IV) and/or Ni(III)/Ni(II), the behaviour can be explained. As $La_{0.99}FeO_3$ contains more Fe(III) than the other samples, this compound will have a high activity towards the reduction of oxygen, if Fe(III) is the most catalytic active specie. The results presented in this study indicates therefore that Fe(III) is the catalytic active specie, in contrast to what sometimes is stated in the literature [24]. For high amounts of Ni, other parameters take over [amount of oxide ion vacancies and the amount of Ni(III)/Ni(II)]. An additional issue could be that the oxide ion vacancies in the pure iron perovskite are disordered, whereas they are ordered in the nickel-containing perovskites due to clustering of the oxide ion vacancies with Ni (II). Another parameter that changes as a function of the amount of Ni is the electronic conductivity (increases with increasing amount of nickel). However, for other systems, it is shown that the electronic conductivity is not rate limiting for the reduction of oxygen [29]; and as the pure iron perovskite has a higher activity than several of the nickel-doped perovskites, this is probably not a rate limiting parameter. It is therefore suggested that Fe(III) (for low amounts of nickel) and oxide ion vacancies (for high amounts of nickel) are the catalytic active species for the reduction of oxygen in this type of perovskites. It should also be noted that on porous planar electrodes, the pure iron perovskite reveals the highest ASR value [11], in contrast to what is observed in this study. There can be at least two reasons for this. In the case of porous symmetrical electrodes, the micro-structure is important for the performance of the electrode. The micro-structure is not important when using cone-shaped electrodes. It could also be due to the low electronic conductivity of the pure iron-based perovskite. This might lead to a low in plane conductivity of the electrodes, which will increase the ASR value of the electrode. In the case of the cone-shaped electrode, there can be corrected for a low electronic conductivity, as explained in this text. This shows that studies on cone-shaped electrodes sometimes give other results than obtained on porous electrodes. On cone-shaped electrodes, the true electro-catalytic properties of the electrode material are revealed. If the ASR values of the LFN cones are compared with measurements on other cone-shaped electrodes, it is observed that the ASR values of $La_{0.99}Fe_{0.4}Ni_{0.6}O_{3-\delta}$ is among the lowest measured [25], even though the ASR values are rather high compared with measurements on porous symmetrical cathodes. It should therefore be noted that studies on cone-shaped electrodes only give relative values. The ASR values obtained on porous symmetrical electrodes are normally lower than the ASR values obtained on cone-shaped electrodes.

The electro-chemical performance of the Fe–Ni-based perovskites evaluated on the background of symmetrical

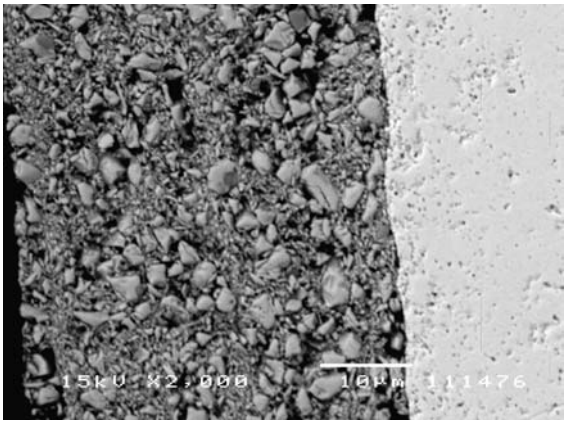

Fig. 6 An SEM micrograph of a composite cathode. It is seen that the cathode consists of two different particles. The small particles as determined with EDS are CGO10. The large particles are then the perovskite phase. This micro-structure explains why the electro-chemical performance of the cathodes is so low. The large particles of the perovskite phase make a percolation pathway of the electronic conducting phase impossible, leading to a low electronic conductivity of the cathode. Especially, a low in-plane conductivity of the cathode might be troublesome

porous electrodes is rather low. This is due to an un-optimised micro-structure, cf. Fig. 6. It is seen that the LFN particles are very large. This means that there is no percolation pathway between the electronic conducting phase, leading to a low in-plane conductivity of the electrode. The powder of LFN perovskites should therefore be made in another way and at a lower calcination temperature to decrease the particle size. One such way could be the glycine–nitrate method [30]. Further work will address this issue. It is possible to lower the ASR values, as the ASR values reported in the literature for porous symmetrical cathodes are much lower than the values found in this study [11].

Conclusion

Six of the $La_{0.99}Fe_{1-x}Ni_xO_{3-\delta}$ perovskites belong to the cubic crystal system as determined by powder XRD, and only the compound $La_{0.99}Fe_{0.4}Ni_{0.6}O_{3-\delta}$ belongs to the hexagonal crystal system. The nickel-containing perovskites have a very high electronic conductivity. The highest conductivity is achieved for the $La_{0.99}Fe_{0.4}Ni_{0.6}O_{3-\delta}$ compound, and the electronic conductivity reaches its maximum at a temperature of 380 °C with the value 670 S/cm. The electro-chemical performance of the nickel-rich, LFN-based perovskites is high, evaluated on the background of measurements on cone-shaped electrodes. The high activity towards the reduction of oxygen of the nickel-rich, Fe–Ni-based perovskites is probably due to a high amount of oxide ion vacancies in the perovskite structure. Furthermore, the TEC of these compounds matches quite well the TEC of the commonly used electrolytes, so the LFN-based perovskites are promising at SOFC cathode materials.

However, due to an un-optimised micro-structure, the performance of the symmetrical porous composite electrodes is rather low. The best symmetrical cathode revealed an ASR value of 0.73 Ωcm^2 at 800 °C.

Acknowledgements Colleagues at the Department of Fuel Cells and Solid State Chemistry are thanked for their encouragement and inspiring discussions. The Danish Energy Agency is thanked for the financial support.

References

1. Minh NQ, Takahashi T (1995) Science and technology of ceramic fuel cells. Elsevier, Amsterdam
2. Minh NQ (1993) J Am Ceram Soc 76:563
3. Xia C, Liu M (2001) Solid State Ion 144:249
4. Xia C, Liu M (2002) Solid State Ion 152:423
5. Liu Y, Rauch W, Zha S, Liu M (2004) Chem Mater 16:3502
6. Liu Y, Rauch W, Zha S, Liu M (2004) Solid State Ion 166:261
7. Sahaibzada M, Benson SJ, Rudkin RA, Kilner JA (1998) Solid State Ion 113–115:285
8. Murray EP, Sever MJ, Barnett SA (2002) Solid State Ion 148:27
9. Shao Z, Haile SM (2004) Nature 431:170
10. Petric A, Huang P, Tietz F (2000) Solid State Ion 135:719
11. Chiba R, Yoshimura F, Sakurai Y (1999) Proceedings of the 6th international symposium on solid oxide fuel cells (SOFC-VI), Honolulu, October 17–22, 1999. In: Singhal SC, Dokiya M (eds). The Electrochemical Society, Pennington, NJ (proceedings volume PV 1999–19), p 453
12. Chiba R, Yoshimura F, Sakurai Y (1999) Solid State Ion 124:281
13. Knudsen J, Friehling PB, Bonanos N (2005) Solid State Ion 176:1563
14. Basu RN, Tietz F, Teller O, Wessel E, Buchkremer HP, Stöver D (2003) J Solid State Electrochem 7:416
15. Bontempi E, Garzella C, Valetti S, Depero LE (2003) J Eur Ceram Soc 23:2135
16. Falcón H, Goeta AE, Ponte G, Carbonio RE (1997) J Solid State Chem 133:379
17. Kharton VV, Viskup AP, Naumivich EN, Tikhonovich VN (1999) Mater Res Bull 34:1311
18. Newman J (1966) J Electrochem Soc 113:501
19. Boukamp BA (1996) 'EQUICVRT'. University of Twente, The Netherlands
20. Goodenough JB, Raccah PM (1965) J Appl Phys 36:1031
21. Torrance JB, Lacorre P, Nazzal AI, Ansaldo EJ, Niedermayer C (1992) Phys Rev B45:8209
22. Mizusaki J, Sasamoto T, Cannon WR, Bowen HK (1983) J Am Ceram Soc 66:247
23. Nitadori T, Misono M (1985) J Catal 93:459
24. Falcon H, Carbonio E (1992) J Electroanal Chem 339:69
25. Kammer K, Mogensen M (2005) Solid state electrochemistry. Proceedings 26 Risø international symposium on materials science, Risø (DK), 4–8 Sept. 2005. In: Linderoth S, Smith A. Bonanos N, Hagen A, Mikkelsen L, Kammer Hansen K, Lybye D, Hendriksen PV, Poulsen FW, Mogensen M, Wang WG (eds). (Risø National Laboratory, Roskilde, 2005), p. 253–260
26. FEMLAB 3.1 (2005) Comsol, Burlington, USA
27. Pedersen T, Saadi S, Nielsen KH, Mørup S, Kammer K (2005) Solid State Ion 176:1555
28. Bucher E, Sitte W (2004) J Electroceram 13:779
29. Kammer K. Solid State Ionics (Accepted for Publication)
30. Chick LA, Pederson LR, Maupin GD, Bates JL, Thomas LE, Exarhos GJ (1990) Mat Lett 10:6